

## Multiple Melting in Segmented Polyurethane Block Copolymers

Jeffrey T. Koberstein\*

*Institute of Materials Science and Department of Chemical Engineering,  
University of Connecticut, Storrs, Connecticut 06269-3136*

Adam F. Galambos

*Himont Research and Development Center, 800 Greenbank Road,  
Wilmington, Delaware 19808*

*Received October 3, 1991; Revised Manuscript Received June 8, 1992*

**ABSTRACT:** Multiple melting in crystallizable segmented polyurethane block copolymers has been investigated by simultaneous synchrotron X-ray-differential scanning calorimetry experiments. Results indicate that the origin of multiple endothermic behavior is dependent on the specimen preparation procedure. In melt-crystallized specimens, multiple endotherms are associated with the melting of two distinct hard segment crystal populations; they have different melting points, but have indistinguishable diffraction patterns consistent with a contracted hard segment crystal form. Compression molding leads to hard segment crystals of an extended form. Multiple melting in compression-molded specimens, observed at low heating rates, is associated with melting-recrystallization-melting of the extended crystalline polymorph into a new poorly-organized hard segment structure. This latter structure transforms into the contracted crystalline polymorph if given sufficient time at an appropriate undercooling. The rate of the polymorphic transition to the contracted polymorph depends strongly on the undercooling and does not occur within the time frame of a typical calorimeter experiment.

## Introduction

Polyurethane elastomers are  $(H_nS_m)_p$  type copolymers comprised of alternating sequences of a glassy or hard (H) material and a rubbery or soft (S) material. The unfavorable interactions between the hard and soft segments drive the system to form a microphase-separated structure which typically imparts elastomeric properties to the polyurethane. Although there exist a countless number of polyurethane formulations varying in monomer type, chemical composition, and properties, one particular class of polyurethanes has been the focus of concerted research efforts. This class of polyurethanes is prepared from 4,4'-methylenediphenyl 1,1'-diisocyanate (MDI), butanediol (BDO), and oligomeric polyglycols (PG) such as poly-(tetramethylene glycol) or poly(propylene glycol) (PPG). The polyglycol forms the soft segment of these polyurethanes, while the hard segment is composed of an altering copolymer of the diisocyanate and the diol chain extender.

One of the most intriguing and perplexing aspects of MDI/BDO/PG polyurethane behavior is the multiple endothermic response evident in their differential scanning calorimetry (DSC) thermograms. Although direct crystallization studies of the neat hard segment have not appeared, the origins of the polyurethane multiple endotherms are generally thought to be associated with the crystallization habits of the MDI/BDO hard segment.

The melting point ( $T_m$ ) characteristics of the endotherms generally fall into two categories: low-temperature endotherms which relate closely to the annealing or crystallization temperature ( $T_c$ ), usually melting about 10–20 °C higher than the temperature at which they form, and high-temperature endotherms which exhibit the behavior of conventional crystallizable homopolymers with folded-chain lamellar morphologies, that is, where  $T_m$  increases linearly with  $T_c$ .

The endothermic response of MDI/BDO polyurethanes is dependent on the procedure for sample preparation as well as the details of subsequent thermal conditioning. Figure 1 illustrates typical melting behavior of MDI/BDO polyurethanes<sup>1</sup> crystallized from the homogeneous melt phase by quenching to  $T_c$ . At low crystallization tem-

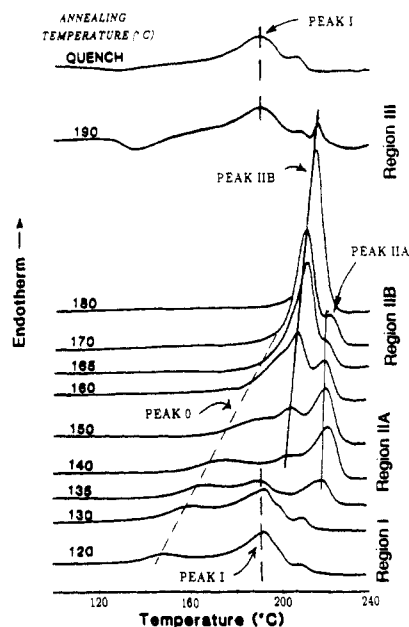


**Figure 1.** DSC thermograms (40 °C/min) of MDI/BDO/PPG polyurethane after melt crystallization at the indicated temperature.<sup>1</sup> The specimen contains 60% by weight of the hard segment.

peratures near the hard segment glass transition (region I), a noncrystalline microphase structure predominates. The high-temperature endotherm in this region (peak I) is associated with a microphase separation transition (MST) to the disordered state (i.e., dissolution of the microphase structure). Thermal conditioning in region II promotes crystallization and the appearance of two high-temperature endotherms. Simultaneous DSC-small-angle X-ray scattering (SAXS) experiments<sup>2</sup> have shown that partial disordering of the microdomain structure occurs during the first high-temperature endotherm (peak IIB) and is followed by complete disordering during the second endotherm (peak IIA). Isothermal crystallization for 1 at temperatures exceeding the MST (i.e., region III) does not produce detectable levels of microphase separation

and/or crystallization. Microphase separation occurs, however, upon cooling the specimen to room temperature and during reheating in the subsequent DSC cycle (as indicated by a phase separation exotherm), leading to melting behavior similar to that observed in region I (see ref 2).

Melt crystallization using a different thermal cycle gives rise to decidedly different behavior. Jacques,<sup>3</sup> for instance, found that crystallization was possible in region III if  $T_c$  was approached from a lower temperature. For example, a specimen which was melted, quenched to form a structure at low temperature, and brought directly up to a higher temperature ( $T_c < T_m$ ) crystallized easily to give structures with melting points that were significantly higher than those obtained by quenching directly down to  $T_c$  from the homogeneous melt temperature. The facilitated crystallization observed for the former thermal cycle may be caused by crystal nuclei which remain after the initial partial melting, and seed the crystallization at higher  $T_c$ . Recently, thermal conditioning of this type (termed solid-melt region annealing) was used to promote a high melting point crystalline structure in a variety of semicrystalline polymers.<sup>4</sup>

Cooper et al.<sup>5,6</sup> have identified three endothermic transitions associated with ordering of the MDI/BDO hard segments in materials subjected to yet a third thermal cycle. The lowest temperature endotherm (60–80 °C) was attributed to the disruption of short-range order of hard segment microdomains. The two high-temperature endotherms were ascribed to the disruption of long-range (120–190 °C) and microcrystalline order (above 200 °C) of the hard microdomains. The samples employed in these studies were compression molded above the highest melting point, slowly cooled under pressure to room temperature, and then thermally postannealed at a temperature below the melting point.

Blackwell and Lee<sup>7</sup> studied multiple melting in MDI polyurethanes that had been oriented and thermally annealed. They found that MDI/BDO hard segments crystallized initially in contracted conformations, but that an extended crystalline polymorph, which has a lower melting point, developed upon elongation and annealing. Conformational analyses<sup>8</sup> have shown that the structure of the extended crystalline polymorph is consistent with an all-trans conformation of the butanediol residue.

Briber and Thomas<sup>9a</sup> reported evidence for two MDI/BDO polymorphs in polyurethanes prepared by solution casting at 145 °C. Crystals termed type I were intrinsically disordered, adopted an extended conformation similar to that reported by Blackwell and Lee, and were associated with nonbirefringent spherulites. Type II crystals formed ordered, birefringent spherulites, exhibited diffraction consistent with the contracted polymorph, and had a higher melting point. In a note added to their original paper,<sup>9b</sup> Briber and Thomas also found evidence for a third polymorph that developed upon stretching. This type III crystal formed by transformation from the type II crystal by annealing under stress. The chain axis reflection for the type III crystal corresponded well with that of the type I structure and was consistent with extended crystal forms with a tilted basal plane.

From the brief review of published work cited above, it is obvious that the melting behavior of MDI/BDO polyurethanes is highly dependent on the procedures adopted for sample preparation. Indeed, the origins of multiple melting may be inherently different for materials prepared under varying conditions. In the present paper, we report studies of multiple melting phenomena in identical

polyurethanes prepared according to two independent procedures: crystallized from the homogeneous melt and compression molded. The crystal structures associated with the various melting endotherms are determined by performing simultaneous DSC–synchrotron X-ray scattering experiments.

## Experimental Section

The series of MDI/BDO materials examined are denoted PU-X, where X refers to the weight percent of hard segment material in the copolymer. The soft segment is poly(oxyethylene-*b*-oxypropylene-*b*-oxyethylene) glycol (PPO-PEO) containing 30.4 wt % oxyethylene end caps. The materials were supplied by Dr. R. Zdrahala of the Union Carbide Corp., and their synthesis has been described elsewhere<sup>10</sup> as have been some of their properties.<sup>1,2,11</sup> Compression-molded specimens were prepared by molding 2-mm-thick plaques in a 1.5-in.-diameter vacuum mold at 180 °C and 3000 psi for 5 min. Prior to molding, the materials were reprecipitated from solutions of the “as-received” polymer in dimethylformamide and then vacuum dried.

The melt-crystallized specimens were prepared by heating a portion of the molded plaque to 240 °C, holding at that temperature for 1 min, cooling to  $T_c$  at a rate of –20 °C/min, holding at  $T_c$  for a prescribed period of time, and cooling to 50 °C at a rate of –20 °C/min. Gel permeation chromatography analysis shows that the molecular weight distribution does not change significantly during this thermal cycle.

Thermal cycling was accomplished with either of two differential scanning calorimeter (DSC) units: a Perkin-Elmer DSC-4, calibrated with indium, cyclohexane, and sapphire standards or, in the case of simultaneous X-ray DSC measurements, a Mettler FP80/84 thermal analysis hot stage.

Conventional wide-angle diffraction (WAXD) profiles were recorded with a Nicolet two-dimensional detector using a Rigaku rotating anode as the source of 0.1542-nm X-rays. Simultaneous WAXD–DSC and small-angle X-ray scattering (SAXS–DSC) measurements were carried out using X-ray radiation (0.143-nm wavelength) on beam line 1–4 at the Stanford Synchrotron Radiation Laboratory. Details regarding the beam line configuration have already been reported.<sup>2,12</sup> The detector is a cooled 1024-channel photodiode array operating at ca. –80 °C. For the purpose of WAXD experiments, the detector is tilted off the incident beam axis by approximately 20°, thereby subtending an angular range of approximately 15–25°.

Thermomechanical analysis was performed using a Perkin-Elmer TMA-LO at a rate of 20 °C/min. The penetration probe load was 10 g, and the instrumental temperature calibration was accomplished using the indium melting point.

## Results

**Melt Crystallization.** In melt crystallization experiments, typified by the thermograms of Figure 1, only one region of crystallization temperatures produced more than one prominent high-temperature endotherm. This region of annealing temperatures was termed region IIA,<sup>1,13</sup> and includes temperatures between 140 and 160 °C (see Figure 1). Melt-crystallized specimens exhibit X-ray diffraction patterns consistent with the type II crystal structure at all annealing temperatures where crystallinity is observed.<sup>13</sup>

DSC thermograms for a polyurethane annealed within this region are shown in Figure 2 as a function of the scan rate. At high scan rates, the shape of the thermogram becomes essentially independent of rate and exhibits two distinct high-temperature endotherms. The lack of rate dependence indicates that the higher temperature endotherm does not form as a result of melting of the first endotherm and recrystallization, but is associated with a distinct crystal population, which is present at the beginning of the DSC scan. The possibility of crystal polymorphism was investigated by performing simultaneous WAXD–DSC measurements. Scattering patterns collected during a DSC scan at a rate of 20 °C/min are

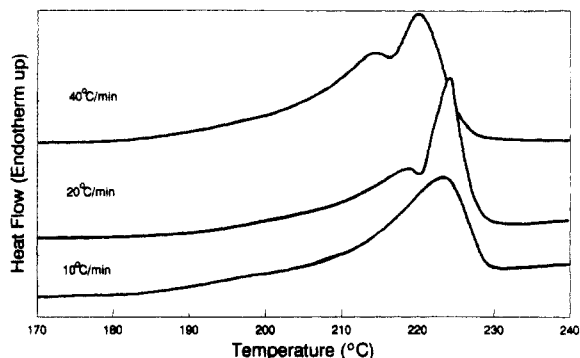


Figure 2. Scan rate dependence of DSC thermograms for PU-60 melt crystallized at 145 °C.

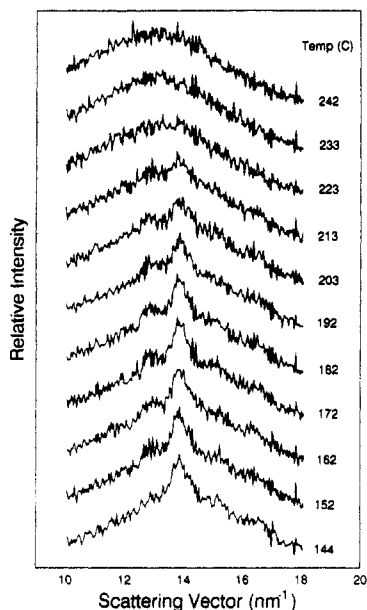


Figure 3. Wide-angle diffraction patterns of PU-60 recorded during a DSC scan at 20 °C/min. The specimen was melt crystallized at 155 °C.

shown in Figure 3. The scattering vector used herein is defined as  $q = (4\pi/\lambda) \sin \theta$ , where  $\lambda$  is the incident X-ray wavelength and  $2\theta$  is the scattering angle. Only one crystal structure is evident throughout the entire temperature cycle even though two distinct endotherms are observed. The lattice spacings derived from the observed reflections are reported in Table I and compared with literature data for similar MDI/BDO polyurethanes. The crystal structure for melt-crystallized PU-60 is consistent with that of the type II or contracted crystal form.<sup>7,9</sup>

The multiple melting behavior is further quantified by determining a relative crystallinity index using a WAXD absolute difference method.<sup>13,14</sup> The crystallinity index data are reported in Figure 4, along with the corresponding DSC thermogram. Three endotherms are observed, corresponding to peak 0, peak IIB, and peak IIA in Figure 1. The crystallinity index remains essentially constant up to ca. 170 °C and then drops off, coincident with the onset of the low-temperature peak 0 endotherm (i.e., the so-called annealing peak). The magnitudes of the crystallinity reduction during each endotherm are commensurate with the associated magnitudes of the enthalpy changes (denoted by the filled circles in Figure 4), indicating that melt recrystallization does not contribute significantly to the observed behavior at this scan rate. At lower scan rates, however, the enthalpy of the peak IIA endotherm becomes enhanced, probably due to melt recrystallization, and a fourth endotherm at even higher temperatures can develop due to melt recrystallization

during the third melting endotherm. Previous simultaneous SAXS-DSC measurements<sup>2</sup> demonstrated that the onset of the highest DSC endotherms was also concurrent with disordering of the hard and soft microphases to form a homogeneous structure. (The low-temperature annealing peak was not observed in the previous work as a result of the thermal cycle employed.) That is, upon melting, the hard segments spontaneously mix with the soft segments. Simultaneous Fourier transform infrared spectroscopy (FTIR)-DSC results,<sup>15</sup> DSC annealing results,<sup>1</sup> and torsion braid analysis experiments<sup>2</sup> provide corroborative evidence for the onset of microphase mixing during these melting endotherms. (More recent SAXS-DSC measurements<sup>13</sup> show that intersegmental mixing increases during all three endotherms.)

The conclusion we reach at the present time is that multiple endotherms when evidenced at high heating rates in melt-crystallized polyurethanes are the result of melting of distinct crystal populations. During each endothermic process, the hard segment crystals not only melt, but also spontaneously mix with the soft microphase. The crystals are not polymorphic, but present apparently identical crystal structures that may be characterized as a contracted type II crystal of MDI/BDO.

Further details pertaining to the origin of the distinct crystal populations, their dependence on crystallization temperature, and their relationship to the kinetics of crystallization and microphase separation will be described in forthcoming publications.

**Compression Molding.** The rate dependence of multiple melting in compression-molded PU-60 is demonstrated by the DSC thermograms presented in Figure 5. In contrast to the response of the melt-crystallized specimen, multiple melting phenomena are apparent in the molded specimens only for low program temperature rates. At high DSC scan rates, only a single melting endotherm is observed, suggesting that the higher temperature endotherm appearing at lower scan rates is related to a melt recrystallization process. The possibility of crystal polymorphism was investigated by recording WAXD scans on samples which were thermally conditioned at a temperature falling between the two endotherms, a procedure employed previously by Blackwell and Lee<sup>6</sup> in studying multiple melting in oriented heat-set elastomers. WAXD profiles were recorded for specimens which had been subjected to three different thermal histories: the as-molded specimen, one that had been heated at 5 °C/min to a temperature (205 °C) within the low-temperature endotherm and then was immediately quenched (-320 °C/min) to room temperature, and one that had been heated at 5 °C/min to a temperature (218 °C) between the two endotherms and quenched. These thermal cycles are illustrated by the corresponding thermograms in Figure 6a. The diffraction pattern for the as-molded specimen (Figure 7) yields lattice spacings consistent with the presence of the type I (i.e., extended) form of MDI/BDO crystals. Similar extended crystal structures were observed for polyurethanes which were deformed during the crystallization process.<sup>8</sup>

The specimen heated to 205 °C exhibits a sharper diffraction maxima (Figure 7) with spacings identical to those of the as-molded material. Thus, during initial melting (i.e., during the low-temperature endotherm), crystals perfect or thicken, but there is no polymorphic crystal transition. The DSC thermogram recorded after the initial thermal cycle (Figure 6b) substantiates this behavior; the heating to 205 °C shifts the initial melting endotherm to higher temperature. The behavior of the

Table I  
Reported Lattice Spacings (Å) for MDI/BDO Crystals

this study melt-crystallized <sup>a</sup>		5.00		4.61	4.43		4.13		3.74	3.47	
this study compression-molded <sup>b</sup>	7.70	4.93	4.77			4.25		3.92		3.59	3.33
this study compression-molded <sup>a</sup>		4.9				4.3		3.9		3.6	
		4.8									
this study compression-molded after annealing at 218 °C <sup>b</sup>	8.6	5.0		4.6			4.1		3.7		
Briber and Thomas <sup>9</sup> type I	7.70	5.01						3.89		3.53	3.33
Briber and Thomas <sup>9</sup> type II	8.6	4.90		4.62	4.45		4.12		3.77	3.49	
Briber and Thomas <sup>9</sup> type III	7.7	5.1					4.12	3.86	3.79	3.56	3.34
		4.99					4.07				
Blackwell et al. <sup>7</sup>	7.65	4.91	4.75	4.60	4.53		4.15	3.89	3.75	3.49	3.30
										3.56	
Born et al. <sup>16</sup>	7.71	4.86				4.25	4.04	3.91		3.55	3.24
Van Bogart, Gibson, and Cooper <sup>17</sup>	8.67	4.93		4.70	4.53		4.17		3.80	3.53	

<sup>a</sup> Synchrotron data have a limited angular range that does not cover the two largest lattice spacings. <sup>b</sup> Data recorded under static conditions on a conventional diffractometer.

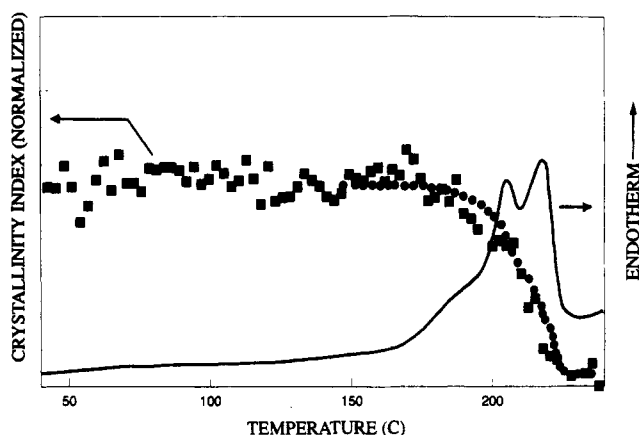


Figure 4. Crystallinity index (from WAXD, squares; from DSC, circles) and DSC thermogram (20 °C/min, for PU-60 crystallized at 155 °C).

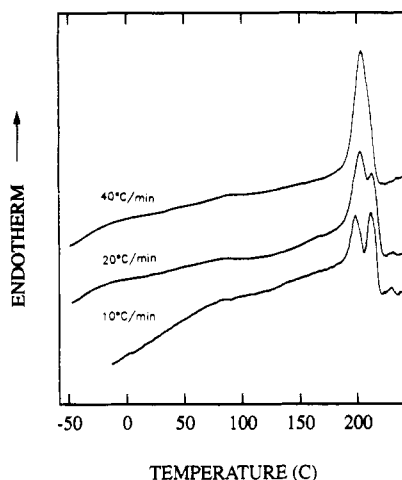


Figure 5. Scan rate dependence of DSC thermograms for compression-molded PU-60.

material heated to 218 °C and cooled to room temperature is quite different. The type I crystalline diffraction pattern is no longer observed. Instead, the diffraction is characteristic of type II contracted crystals, indicating that a polymorphic crystal transition has occurred during this thermal history. This crystal transformation is clearly visible in Figure 7 as a shift in the low-angle spacings. The type I extended crystal has a *c*-axis reflection at ca. 8.04 nm<sup>-1</sup> corresponding to a spacing<sup>7,9,16</sup> of 0.77 nm. After annealing at 218 °C, this reflection shifts to a lower scattering vector corresponding to a spacing of ca. 0.86 nm, characteristic of the type II contracted crystal.<sup>9,17</sup> In addition, the 15.8-nm<sup>-1</sup> reflection (0.39 nm spacing) is replaced by two new reflections corresponding to spacings

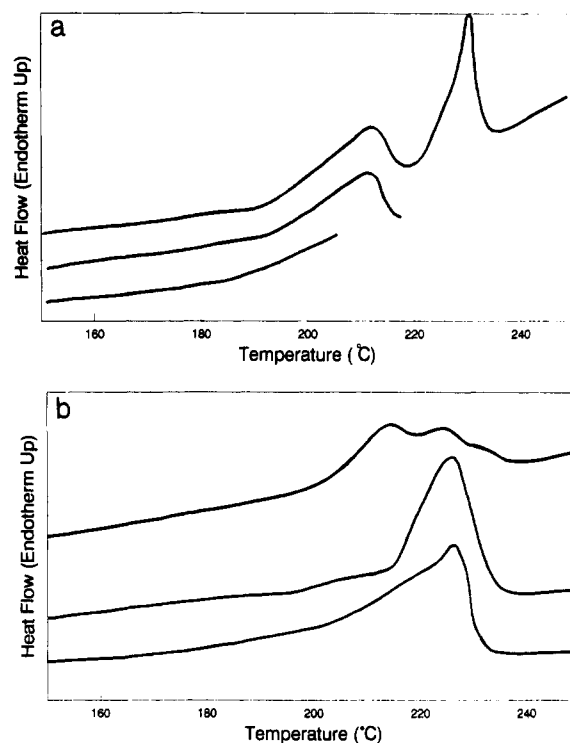
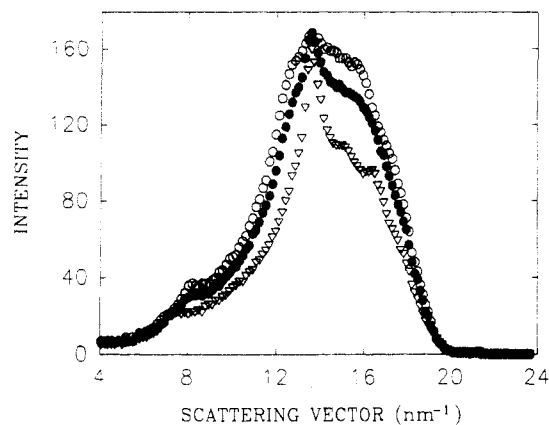


Figure 6. (a) DSC thermograms for compression-molded PU-60: specimen heated to 205 °C (top); specimen heated to 218 °C (middle); full thermogram (bottom) of as-molded specimen. (b) DSC thermograms of PU-60 (40 °C/min) after thermal processing: specimen heated to 205 °C (middle); specimen heated to 208 °C (top); as-molded specimen (bottom).

of 0.37 nm and 0.41 nm, characteristic of a type I to type II crystal transition (see Table I for a compiled listing of reflections). The corresponding DSC thermogram (Figure 6b) exhibits a corresponding shift to a lower melting point characteristic of the contracted polymorph. Part of the higher temperature endotherm remains, even though the diffraction pattern of the extended polymorph is not detectable. This result suggests that the transformation may not be complete.

The appearance of the new crystal form was also investigated with the aid of simultaneous WAXD-DSC measurements. The resultant diffraction patterns for compression-molded PU-60 recorded during a DSC scan at 20 and 2 °C/min are shown in Figures 8 and 9. At room temperature, the observed lattice spacings are consistent with the presence of MDI/BDO crystals with the extended or type I structure (see Table I). During heating at both rates, the diffraction fingerprint of the type I, extended MDI/BDO crystals gradually disappears. New diffraction peaks are not observed, either during, or after, the first



**Figure 7.** WAXD profiles (at room temperature) for compression-molded PU-60: specimen after heating to 205 °C (filled circles); specimen after heating to 218 °C (open triangles); as-molded specimen (open circles).

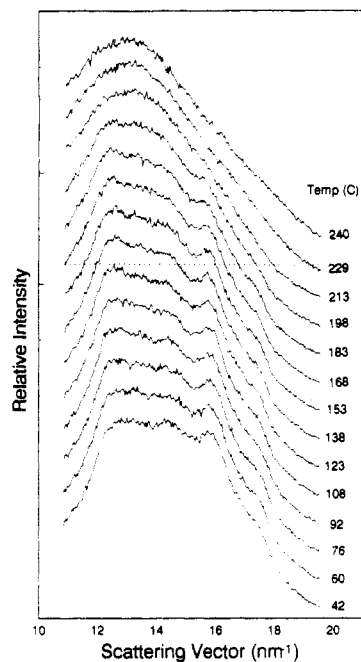


**Figure 8.** WAXD profiles for compression-molded PU-60 recorded during a DSC scan at 20 °C/min.

melting endotherm that might be ascribed to the polymorphic transition from extended to contracted crystals implied by the results of the partial melting static diffraction experiments discussed earlier. The sample that was heated to 218 °C and quenched to room temperature clearly contained contracted crystals (Figure 7). During the actual temperature scan, however, there is no suggestion of crystal transformation. The second, higher temperature endotherm cannot be ascribed therefore to the melting of contracted type II crystals, but must be associated with the disruption of some new poorly-organized structure.

At a lower scan ratio of 2 °C/min, a polymorphic crystal transition is still not observed, as indicated by the diffraction patterns in Figure 9. The contracted type II crystal does form upon cooling after the first DSC cycle (Figure 10), providing an explanation for the static WAXD result, and will also form eventually for specimens held at a temperature intermediate between the two endotherms (Figure 11). These WAXD profiles are identical to those observed for the melt-crystallized specimens.

Recrystallization of the melted type I extended crystals into the type II contracted crystals apparently is not rapid enough to form significant type II crystallinity during a

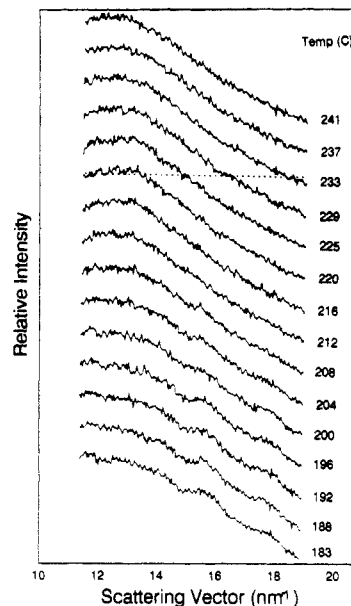


**Figure 9.** WAXD profiles for compression-molded PU-60 recorded during a DSC scan at 2 °C/min.

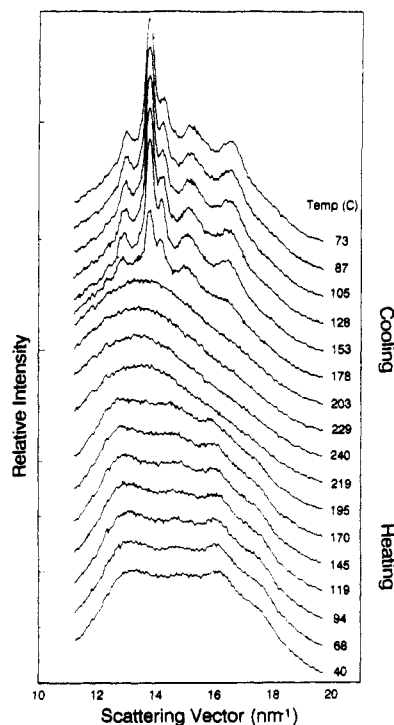


**Figure 10.** WAXD profiles for compression-molded PU-80 recorded during a DSC scan at 20 °C/min, and subsequent controlled cooling.

normal DSC temperature program cycle. Multiple melting in compression-molded polyurethanes therefore appears to be the result of a melt recrystallization process rather than a crystal-crystal transformation. As the extended crystal form melts, the resultant nuclei reside in a supercooled melt. They then crystallize in similar fashion to the melt-crystallized specimens and therefore exhibit a contracted type II crystallization habit. The rate of type II recrystallization is a strong function of the undercooling, however, such that recrystallization to an ordered crystal cannot take place at normal DSC temperature program rates but does occur rapidly upon cooling to room temperature. Only a weak diffraction shoulder is observed above the first melting endotherm suggestive of a poorly organized, perhaps liquid crystalline structure which

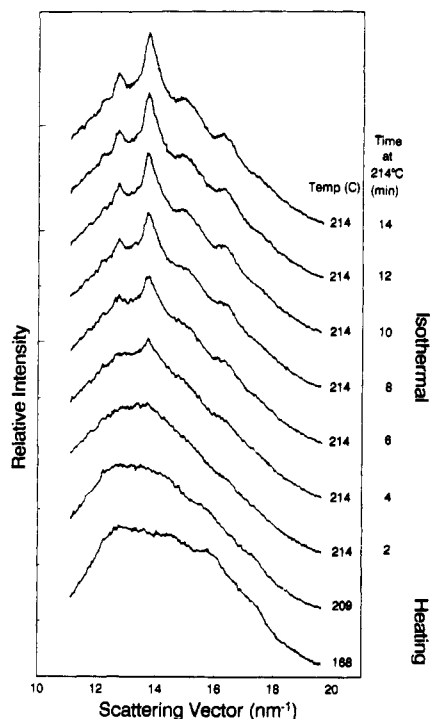


**Figure 11.** Time dependence of WAXD for compression-molded PU-70 heated to 214 °C and held at that temperature.

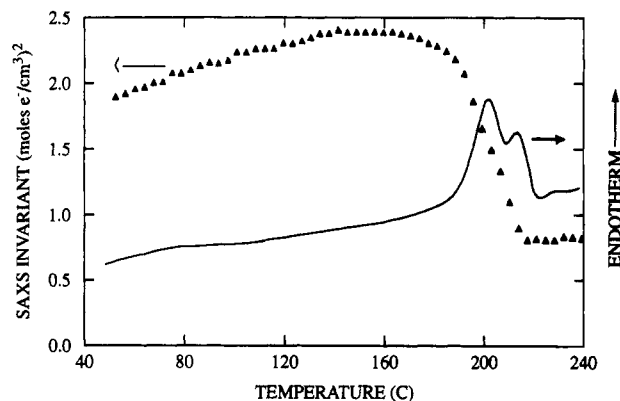


**Figure 12.** Small-angle X-ray scattering invariant (triangles) and DSC thermogram (line) for compression-molded PU-60 recorded at 10 and 20 °C/min, respectively.

disorders during the second higher temperature endotherm.

The hypothesis that a portion of the hard segments are still associated into some microphase structure after the first melting endotherm is supported by data from simultaneous SAXS-DSC experiments. The SAXS invariant data (a measure of the degree of microphase separation<sup>14</sup>) is reported as a function of the program temperature in Figure 12. As in the case of the melt-crystallized specimens, some of the hard segments that melt during the first endotherm spontaneously mix with the soft segments, thereby decreasing the overall degree of microphase separation (i.e., the volume fraction of segregated hard segments). This decrease is indicated by the drop in the invariant during the first endotherm (Figure 12). The invariant is still finite after the first endotherm, demonstrating that some of the hard segments are still associated at 218 °C. Only after melting out the second endotherm does the invariant fall to zero as the structure becomes completely disordered. Only a certain fraction of the extended crystalline material reforms into the poorly-organized hard microdomains that dissociate during the second endotherm. The remaining fraction spontaneously mixes with the soft segments upon melting as

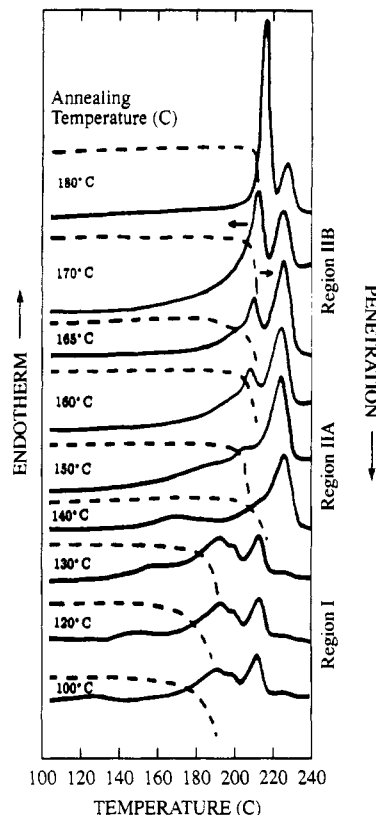


**Figure 13.** TMA softening curves (dashed lines) and DSC thermograms (solid lines) for compression-molded polyurethanes (20 °C/min).

reflected by the decrease in the SAXS invariant during the first endotherm. This mixing occurs since the temperature under these conditions exceeds the microphase stability or order-disorder transition temperature (i.e., MST).

The hypothesis that the polymorphic crystal transition is incomplete, that is, that during the temperature program all of the extended crystalline hard segment material does not reform into a new associated structure, is supported by the thermomechanical data presented in Figure 13. As can be seen from the data, the softening point is coincident with melting of the Type I extended crystals and occurs prior to melting of the second endotherm. The amount of transformation to the higher melting endotherm therefore appears to be insufficient to form a continuous hard segment network capable of supporting appreciable stress.

## Summary

The origins of multiple endotherms in differential scanning calorimeter thermograms of segmented polyurethane block copolymers with crystallizable MDI/BDO hard segments have been studied by simultaneous X-ray-DSC measurements. In melt-crystallized specimens, multiple endotherms are associated with distinct crystal populations with different melting points, but with indistinguishable crystalline diffraction patterns, consistent with hard segment crystals of a contracted form. During each endotherm, the hard segment material that melts spontaneously mixes with the soft segment microphase, since this temperature exceeds the microphase order-disorder temperature.

Multiple melting in compression-molded specimens results from melt recrystallization processes. At high DSC temperature program rates, only a single endotherm is observed. The crystal structure that melts during this endotherm is determined to be an extended crystal form.

At lower program rates, a portion of the hard segment material that melts during the first endotherm recrystallizes into a poorly organized structure which subsequently melts during a second higher temperature endotherm. The poorly-organized structure will transform into the contracted crystalline form observed for the melt-crystallized specimens if held isothermally for a sufficient period of time or upon cooling. The origin of multiple melting in polyurethanes is therefore dependent upon the specimen preparation procedure.

**Acknowledgment.** Some of the materials incorporated in this work were developed at the Stanford Synchrotron Radiation Laboratory with the financial support of the National Science Foundation (Grant DMR-77-27489) in cooperation with the Department of Energy. Partial support for this research was provided by a grant from the Office of Naval Research. We acknowledge Dr. T. P. Russell for assisting in collecting the synchrotron X-ray data and Ms. W. Hu and Dr. J. Gromek for measurement of the static WAXD profiles.

## References and Notes

- (1) Leung, L. M.; Koberstein, J. T. *Macromolecules* **1986**, *19*, 706.
- (2) Koberstein, J. T.; Russell, T. P. *Macromolecules* **1986**, *19*, 714.
- (3) Jacques, C. H. M. In *Polymer Alloys*; Klempner, D., Frisch, K. C., Eds.; Plenum Press: New York, 1977; p 287.
- (4) Khanna, Y. P.; Kumar, R. *J. Polym. Sci., Polym. Phys. Ed.* **1989**, *27*, 369.
- (5) Hesketh, T. R.; Van Bogart, J. W. C.; Cooper, S. L. *Polym. Eng. Sci.* **1980**, *20*, 190.
- (6) Van Bogart, J. W. C.; Bluemke, D. A.; Cooper, S. L. *Polymer* **1981**, *22*, 1428.
- (7) Blackwell, J.; Lee, C. D. *J. Polym. Sci., Polym. Phys. Ed.* **1984**, *22*, 759.
- (8) Blackwell, J.; Nagarajan, M. R. *Polymer* **1981**, *22*, 202.
- (9) (a) Briber, R. M.; Thomas, E. L. *J. Macromol. Sci., Phys.* **1983**, *B22*, 509. (b) Briber, R. M.; Thomas, E. L. *J. Polym. Sci., Polym. Phys. Ed.* **1985**, *23*, 1915.
- (10) Zdrahala, R. J.; Critchfield, F. E.; Gerkin, R. M.; Hager, S. L. *J. Elastomers Plast.* **1980**, *12*, 184.
- (11) Leung, L. M.; Koberstein, J. T. *J. Polym. Sci., Polym. Phys. Ed.* **1985**, *23*, 1883.
- (12) Stephenson, G. B. Ph.D. Dissertation, Stanford University, 1982 (Report No. 82/05; Stanford Synchrotron Radiation Laboratory: Stanford, CA).
- (13) Galambos, A. F. Ph.D. Dissertation, Princeton University 1989.
- (14) Alexander, L. E. *X-Ray Diffraction Methods in Polymer Science*; Wiley-Interscience: New York, 1969.
- (15) Koberstein, J. T.; Gancarz, I.; Clarke, T. *J. Polym. Sci., Polym. Phys. Ed.* **1986**, *24*, 2487.
- (16) Born, L.; Crone, J.; Hespe, H.; Müller, R. H.; Wolf, K. H. *J. Polym. Sci., Polym. Phys. Ed.* **1984**, *22*, 163.
- (17) van Bogart, J. W. C.; Gibson, P. E.; Cooper, S. L. *J. Polym. Sci., Polym. Phys. Ed.* **1983**, *21*, 65.

**Registry No.** (MDI)(BDO)(PPO)(PEO) (block copolymer), 111938-02-4; (MDI)(BDO)(PPG) (block copolymer), 143077-61-6.